

Study of Cosmic Evolution admitting Thermodynamic Analysis

M. Sharif ^{*}, M. Zeeshan Gul [†] and Nusrat Fatima [‡]

Department of Mathematics and Statistics, The University of Lahore,
1-KM Defence Road Lahore-54000, Pakistan.

Abstract

This article examines the cosmic evolution in the framework of symmetric teleparallel theory, characterized by the function of non-metricity scalar (Q). We use the e-folding number and reconstruction method with a suitable parametrization of the scale factor to obtain the functional form of symmetric teleparallel theory. Using this reconstructed model, we examine the behavior of different cosmographic parameters to demonstrate the bouncing scenarios of the cosmos by considering the contraction and expansion phases of cosmos before and after the bouncing point, respectively. It is found that the null energy condition is violated which shows that the singularity issue can be resolved in this extended theoretical framework. Moreover, we observe that the acceleration occurs near the bouncing point and the reconstructed model aligns with the current cosmic expansion. Finally, we check the validity of second law of thermodynamics in the bouncing framework of our model.

Keywords: Bounce models; Modified theory; Cosmological parameters.

PACS: 64.30.+t; 04.20.Dw; 04.50.kd.

^{*}msharif.math@pu.edu.pk

[†]mzeeshangul.math@gmail.com

[‡]nusratfatimaliaqat@gmail.com

1 Introduction

The current accelerated expansion of the cosmos has been a captivating and significant discovery for researchers over the past two decades. Scientists claimed that this cosmic expansion is driven by a mysterious force, known as dark energy (DE). Cosmologists have been motivated to investigate the elusive nature of this enigmatic energy. To account the puzzling features of DE, Einstein introduced the cosmological constant into his field equations, known as Λ CDM model. However, this model faces two primary challenges, i.e., the coincidence problem and the fine-tuning problem. The coincidence problem arises from the notable discrepancy between the observed and predicted values of energy density. Another question is why we are observing the current cosmic acceleration when the energy densities of dark matter and DE are assumed to be equal [1]. To address these problems and unveil the cosmic mysteries, various modified gravitational theories (MGTs) such as curvature-based, torsion-based and non-metricity-based theories have been developed [2]-[16]. One of the well-known approaches to discuss the dark universe is $f(\mathcal{Q})$ gravity, where the gravitational Lagrangian involves a generic function of the non-metricity [17].

The study of $f(\mathcal{Q})$ theory has gained significant interest in recent times due to its consistency with observational data and its implications for cosmology. Researchers have investigated various aspects of this theoretical framework. Lazkoz et al [18] studied the cosmic evolution using redshift function in this theory. Jimenez et al [19] examined the cosmic perturbations in this modified framework. Mandal and his colleagues [20] examined the energy conditions (ECs) to evaluate the viability of cosmological models in the same theoretical context. Bajardi et al [21] utilized the Hamiltonian approach to derive the cosmic wave function. Hassan et al [22] explored the stability analysis of wormhole solutions in the symmetric teleparallel theory. Solanki et al [23] investigated the role of bulk viscosity in the cosmic accelerated expansion. Esposito et al [24] used reconstruction techniques to study the precise isotropic and anisotropic cosmological solutions. Arora and Sahoo [25] looked into the cosmic evolution through the EoS parameter. Albuquerque and Frusciante [26] examined the evolution of linear perturbations in the same theory. Sokoliuk et al [27] explored the evolution of the universe using Pantheon data sets. Khylllep et al [28] analyzed the cosmic expansion employing power-law and exponential forms of this gravity to understand the cosmic dynamics. The geometry of compact stars with different considera-

tions in $f(\mathcal{Q})$ and $f(\mathcal{Q}, T)$ theory has been studied in [29]-[35], where T is the trace of the energy momentum tensor (EMT). The $f(\mathcal{Q})$ gravity models in a Friedmann-Robertson-Walker (FRW) and Bianchi type-I spacetimes provide valuable insights into the role of non-metricity in gravitational effects and cosmological scenarios [36]-[37].

Cosmological observations indicate that the universe originated from a singularity, known as the big bang. However, this theory faces several issues such as the horizon and flatness problems. To address these problems, the inflation theory was developed which provides a basic explanation for cosmic expansion. While the inflation theory [38] successfully resolves many issues but it fails to address the initial singularity problem. In this regard, a viable cosmic model called bouncing cosmology has been proposed to resolve the initial singularity. The bounce theory describes a cyclic pattern where the collapse of one cosmic event precedes the occurrence of a new one. During this bouncing cosmological behavior, the Hubble parameter shows the transitions from contraction to expansion phases. Bounce solutions are significant in cosmology as they offer a way to solve the initial singularity problem.

Bouncing cosmology in MGTs has attracted significant interest because of their intriguing features. Barragan et al [39] examined bouncing cosmology in Palatini $f(R)$ gravity. Saaidi et al [40] used the Bianchi type-I space-time to analyze cosmic evolution in $f(R)$ framework. Jawad and Rani [41] studied cosmic evolution through a generalized ghost DE model in the same work. Shabani and Ziaie [42] investigated non-singular bouncing solutions with perfect matter configuration in $f(R, T)$ framework. Aly [43] studied the generalized second law of thermodynamics in the background of Ricci DE models, examining both interacting and non-interacting scenarios. Malik and Shamir [44] explored the bouncing cosmos in the same theory and found that specific solutions can accommodate exotic matter. Shekh [45] used the second law of thermodynamic to analyze the dynamical behavior of anisotropic DE models in the framework of $f(R, G)$ theory, where G is the Gauss-Bonnet invariant. Ilyas et al [46] studied the cosmic dynamics through different $f(R)$ models and observed that these models can resolve the initial singularity. Zubair et al [47] discussed the viability of the reconstructed cosmic models in $f(R, T)$ theory. Bhardwaj et al [48] examined cosmic evolution using cosmographic parameters in the same framework. Lohakare et al [49] used $f(R, G)$ gravity models to analyze the bouncing cosmos. Dimakis et al [50] studied viable anisotropic solutions for Kantowski-Sachs and Bianchi type-III spacetimes in $f(\mathcal{Q})$ theory. The analysis of observational constraints

in MGTs has also been explored in various studies [51]-[54]. Sharif et al [55] studied the cosmic bounce in non-Riemannian geometry. Sharif and his collaborators studied the Noether symmetry approach [56]-[59], stability of the Einstein universe [60]-[61], dynamics of gravitational collapse [62]-[63] and static spherically symmetric structures [64]-[67] in $f(R, T^2)$ theory.

This manuscript provides a framework to study the cosmic evolution with thermodynamic analysis in $f(\mathcal{Q})$ theory. The paper is organized in the following order. In section 2, we define the vacuum action in $f(\mathcal{Q})$ gravity and use the reconstruction technique to find the functional form of modified symmetric teleparallel theory. Also, we derive the field equations of $f(\mathcal{Q})$ gravity in the presence of FRW spacetime. The comprehensive analysis of the bouncing universe is presented in the section 3. Additionally, we use the reconstructed functional form of $f(\mathcal{Q})$ to discuss the graphical behavior of cosmic parameters. The brief analysis of the second law of thermodynamics is provided in section 4. Our main findings are summarized in the section 5.

2 Reconstructed $f(\mathcal{Q})$ Functional Form

The modified action of $f(\mathcal{Q})$ gravity in vacuum is given by

$$\mathcal{S} = \frac{1}{2\kappa} \int f(\mathcal{Q}) \sqrt{-g} d^4x, \quad (1)$$

where $\kappa = 1$ represents the coupling constant and g denotes the determinant of the metric tensor. In the integrand, the non-metricity is given by (detailed calculation is given in Appendix X)

$$\mathcal{Q} = -\mathcal{Q}_{\xi\alpha\beta} \mathcal{P}^{\xi\alpha\beta} = -\frac{1}{4}(-\mathcal{Q}^{\xi\alpha\beta} \mathcal{Q}_{\xi\alpha\beta} + 2\mathcal{Q}^{\xi\alpha\beta} \mathcal{Q}_{\beta\xi\alpha} - 2\mathcal{Q}^\xi \tilde{\mathcal{Q}}_\xi + \mathcal{Q}^\xi \mathcal{Q}_\xi), \quad (2)$$

where

$$\mathcal{P}^\xi_{\alpha\beta} = -\frac{1}{2}L^\xi_{\alpha\beta} + \frac{1}{4}(\mathcal{Q}^\xi - \tilde{\mathcal{Q}}^\xi)g_{\alpha\beta} - \frac{1}{4}\delta^\xi_{(\alpha} \mathcal{Q}_{\beta)}, \quad (3)$$

and

$$\mathcal{Q}_\xi \equiv \mathcal{Q}^\alpha_{\xi\alpha}, \quad \tilde{\mathcal{Q}}_\xi \equiv \mathcal{Q}^\alpha_{\xi\alpha}. \quad (4)$$

To derive the gravitational field equations, one can perform a variation of the action with respect to the metric tensor. The explicit formulation of $\delta\mathcal{Q}$ is provided in Appendix Y. We consider a flat FRW metric as

$$ds^2 = -dt^2 + (dx^2 + dy^2 + dz^2)a^2(t), \quad (5)$$

where $a(t)$ is the scale factor. The gravitational field equations can be obtained as

$$3H^2 = \frac{1}{2}f - 6H^2f_{\mathcal{Q}}, \quad (6)$$

$$2\dot{H} + 3H^2 = 2f_{\mathcal{Q}}\dot{H} + 2f_{\mathcal{Q}\mathcal{Q}}H + 6f_{\mathcal{Q}}H^2 - \frac{1}{2}f. \quad (7)$$

Here, $f(\mathcal{Q}) \equiv f$, $f_{\mathcal{Q}} = \frac{\partial f}{\partial \mathcal{Q}}$ and dot is the time derivative. Using Eqs.(2) and (5), the value of non-metricity turns out to be (details are given in Appendix **Z**)

$$\mathcal{Q} = 6H^2. \quad (8)$$

Since the solution of the field equations (6) and (7) is very complicated as they contain multi-variables and their derivatives. Thus, we use the reconstruction method to address this problem and calculate the value of $f(\mathcal{Q})$. In this method, the Hubble parameter is known. Firstly, the gravitational field can be described by the e-folding number ($\mathcal{N} = \ln(\frac{a}{a_0})$) and simplification of the resulting second order differential equation allows us to deduce the value of $f(\mathcal{Q})$. Thus, Eq.(8) in terms of e-folding number becomes

$$\mathcal{Q}(\mathcal{N}) = 6H^2(\mathcal{N}). \quad (9)$$

To reduce the complexity, we assume the particular form of Hubble parameter as [68]

$$H^2(\mathcal{N}) = P(\mathcal{N}) \Rightarrow \mathcal{Q}(\mathcal{N}) = 6P(\mathcal{N}). \quad (10)$$

We assume the cosmic scale factor as [69]

$$a(t) = (1 + \mu t^2)^{\frac{\nu}{2}}, \quad (11)$$

where μ and ν are positive parameters. The Hubble parameter and e-folding number associated to this scale factor turn out to be

$$H = \frac{\dot{a}}{a} = \frac{\mu\nu t}{1 + \mu t^2}, \quad \mathcal{N} = -\frac{\nu}{2} \ln\left(\frac{\mathcal{Q}}{6\mu\nu^2}\right). \quad (12)$$

Using e-folding number relation, we obtain

$$H^2(\mathcal{N}) = P(\mathcal{N}) = \mu\nu^2 e^{\frac{-2\mathcal{N}}{\nu}}. \quad (13)$$

Using Eq.(10) in (7), it follows that

$$\frac{P'(\mathcal{N})}{\sqrt{P(\mathcal{N})}} - \frac{P'(\mathcal{N})f_{\mathcal{Q}}}{\sqrt{P(\mathcal{N})}} - \frac{12P(\mathcal{N})f_{\mathcal{Q}\mathcal{Q}}}{\sqrt{P(\mathcal{N})}} - \frac{f}{2} + 6P(\mathcal{N})f_{\mathcal{Q}} + 3P(\mathcal{N}) = 0. \quad (14)$$

The solution of this differential equation is

$$\begin{aligned} f(\mathcal{Q}) = & c_1 e^{\frac{\mathcal{Q}(-P'(\mathcal{N}) - \sqrt{P'^2(\mathcal{N}) - 24P^{3/2}(\mathcal{N})})}{24P(\mathcal{N})}} + c_2 e^{\frac{\mathcal{Q}(-P'(\mathcal{N}) + \sqrt{P'^2(\mathcal{N}) - 24P^{3/2}(\mathcal{N})})}{24P(\mathcal{N})}} \\ & + 2 \frac{P'(\mathcal{N}) + 3P^{3/2}(\mathcal{N})}{\sqrt{P(\mathcal{N})}}, \end{aligned} \quad (15)$$

where c_1 and c_2 are the integration constants and prime is the derivative corresponding to e-folding number. In the upcoming sections, cosmological parameters will be discussed with the help of this obtained $f(\mathcal{Q})$ function.

The general integral action of the $f(\mathcal{Q})$ theory is specified as follows [70]

$$\mathcal{S} = \int \left(\frac{1}{2\kappa} f(\mathcal{Q}) + L_m \right) \sqrt{-g} d^4x. \quad (16)$$

Here, L_m denotes the Lagrangian density associated with matter. The associated field equations are

$$\frac{2}{\sqrt{-g}} \nabla_{\xi} (f_{\mathcal{Q}} \sqrt{-g} \mathcal{P}_{\alpha\beta}^{\xi}) + \frac{1}{2} f g_{\alpha\beta} + f_{\mathcal{Q}} (\mathcal{P}_{\alpha\xi\tau} \mathcal{Q}_{\beta}^{\xi\tau} - 2 \mathcal{Q}^{\xi\tau}{}_{\alpha} \mathcal{P}_{\xi\tau\beta}) = T_{\alpha\beta}. \quad (17)$$

Here, ∇_{ξ} demonstrates the covariant derivative and $T_{\alpha\beta}$ denotes the EMT. We consider the perfect fluid configuration as

$$T_{\alpha\beta} = (p_m + \rho_m) u_{\alpha} u_{\beta} + p_m g_{\alpha\beta}, \quad (18)$$

where p_m is the pressure, ρ_m is the energy density and u_{α} is the four-velocity of the fluid. The resulting field equations in the background of the flat FRW spacetime metric turn out to be

$$\rho_m = \frac{1}{2} f - 6H^2 f', \quad (19)$$

$$p_m = 2f' \dot{H} + 2f'' H + 6f' H^2 - \frac{1}{2} f. \quad (20)$$

These field equations are useful for analyzing the complex nature of the cosmos. Banerjee et al [71] examined different forms of non-metricity to examine the mysterious universe.

3 Bouncing Cosmology in $f(Q)$ Theory

Bouncing cosmology offers a different perspective from the big bang theory by proposing that the universe experiences periods of contraction and expansion with a bounce. In the field of cosmology, bouncing solutions are important as they address the initial singularity associated with the cosmic expansion. Consequently, they provide an alternative explanation to the big bang singularity. In a cyclic universe, the cosmos transits from a previous contraction phase to an expansion phase without encountering a singularity. The cosmic bounce can be seen as a rhythmic or periodic occurrence where the collapse of one phase leads to another cosmological event. Cai and his colleagues [72] examined the bouncing universe to develop a non-singular bounce scenario following a contraction phase. The following conditions must be satisfied for the viable non-singular bouncing universe.

- The scale factor must be at its minimum close to the bounce point for a nonsingular bouncing model. The decreasing behavior of scale factor indicates that the universe is in contracting phase, while its increasing behavior signifies a period of cosmic expansion.
- The universe experiences contraction and expansion phases when Hubble parameter is positive and negative, respectively. The bounce point is obtained at $H = 0$.
- The universe passes through an accelerating phase when deceleration parameter is negative and the cosmos undergoes in an expansion era when the deceleration parameter is positive.
- The EoS parameter describes the universe entering a phantom stage when $\omega < -1$ and a quintessence phase when $-1/3 < \omega < -1$.
- The energy density must be positive, finite as well as maximum and pressure should be negative for the existence of non-singular bounce.
- In the case of a non-singular bouncing universe, the ECs must be violated.

These constraints have implications to our comprehension of the early universe and serve as observable indicators of bouncing scenarios. Therefore, these characteristics provide further insight into the fundamental properties of the cosmos.

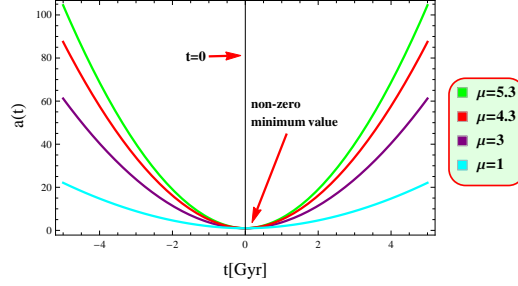


Figure 1: Behavior of scale factor for different values of μ and $\nu = 1.9$.

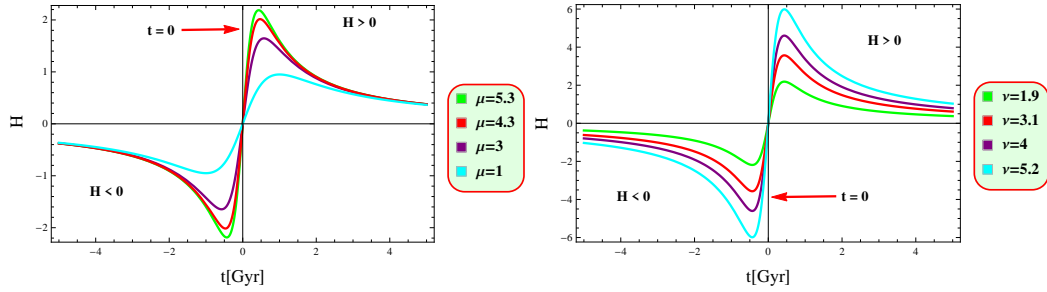


Figure 2: Behavior of Hubble parameter for different parametric values.

3.1 Evolution of the Scale Factor

The behavior of scale factor is crucial in understanding the dynamics of the expanding, contracting and bouncing universe. It is a positive function that changes over time and used to quantify the expansion of the universe and its size. However, the cosmic time is measured in gigayears (Gyr). The expression for the scale factor is given in Eq.(11). The graphical representation of scale factor is shown in Figure 1, which shows its decreasing nature leading to the smallest value (non-zero) and then increasing, providing an explanation for the bouncing pattern observed in the initial phases of cosmic development. From this plot, it is clear that the cosmos is shifted from a contracting phase to an expanding phase. Furthermore, it indicates that the scale factor grows symmetrically around the bouncing point.

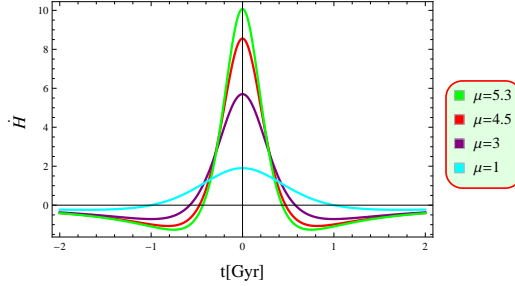


Figure 3: Evolution of temporal derivative of Hubble parameter.

3.2 Dynamics of Hubble Parameter

Now, we use the Hubble parameter to investigate the behavior of cosmos and other cosmic applications. The Hubble parameter corresponding to the scale factor is shown in Eq.(12). This parametrization is designed to model a bouncing universe scenario, which helps in understanding cosmic acceleration. Figure 2 shows a transition from a contracting to an expanding universe as H becomes negative before the bounce point and positive after the bounce for different values of μ and ν . Moreover, the negative values for model parameters do not support the cosmic acceleration.

The nature of Hubble parameter is shown in Tables 1 and 2 for various values of μ and ν , respectively. The behavior of the Hubble constant with different values of μ is shown in Table 1 while keeping $\nu = 1.9$. Table 2 analyzes how the Hubble parameter evolves with different values of ν by keeping μ constant at 5.3. Figure 3 shows that the time derivative of the Hubble parameter is positive near the bounce point for different values of μ , which demonstrates the cosmic acceleration.

3.3 Analysis of Rate of Cosmic Expansion

The rate of expansion is determined by the deceleration parameter, i.e., the positive value indicates an decelerated cosmos whereas a negative value demonstrates an accelerated universe. This parameter is expressed as

$$q = -\frac{\dot{H}}{H^2} - 1 = \frac{t^2\mu - 1 - t^2\mu\nu}{t^2\mu\nu}. \quad (21)$$

Table 1: **Nature of Hubble Parameter for different values of μ** ($\nu = 1.9$).

μ	Time Interval	Behavior of H	Nature of Cosmos
5.3	$-0.5 < t < 0$	$H < 0$	Contraction
4.5	$-0.5 < t < 0$	$H < 0$	Contraction
3	$-0.5 < t < 0$	$H < 0$	Contraction
1	$-0.5 < t < 0$	$H < 0$	Contraction
5.3	$0 < t < 0.5$	$H > 0$	Expansion
4.5	$0 < t < 0.5$	$H > 0$	Expansion
3	$0 < t < 0.5$	$H > 0$	Expansion
1	$0 < t < 0.5$	$H > 0$	Expansion

Table 2: **Nature of Hubble Parameter for different values of ν** ($\mu = 5.3$).

ν	Time Interval	Behavior of H	Nature of Cosmos
1.9	$-0.5 < t < 0$	$H < 0$	Contraction
3.1	$-0.5 < t < 0$	$H < 0$	Contraction
4	$-0.5 < t < 0$	$H < 0$	Contraction
5.2	$-0.5 < t < 0$	$H < 0$	Contraction
1.9	$0 < t < 0.5$	$H > 0$	Expansion
3.1	$0 < t < 0.5$	$H > 0$	Expansion
4	$0 < t < 0.5$	$H > 0$	Expansion
5.2	$0 < t < 0.5$	$H > 0$	Expansion

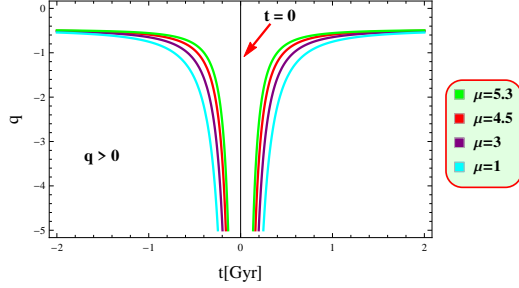


Figure 4: Nature of deceleration parameter versus cosmic time.

The graphical behavior of deceleration parameter is shown in Figure 4, which determines that the universe is in the accelerated expansion phase as the value of deceleration parameter is negative.

3.4 Evolution of Matter Variables

In this subsection, we examine the impact of the reconstructed functional form of $f(\mathcal{Q})$ given in Eq.(17) on the dynamics of the cosmic bounce using matter variables. The incorporation of additional terms may yield beneficial outcomes. The reconstructed functional form provides a streamlined approach to observe the influences of energy density and pressure on diverse cosmic phenomena. The units for energy density and pressure are considered as GeV/cm^3 . Using the value of model in Eqs.(19) and (20), we get

$$\begin{aligned} \rho_m &= \frac{1}{24(1+\mu t^2)^2 \mu \nu^2} \left[\Upsilon_1((1+\mu t^2)^2 + 12(6\mu\nu - 1)\mu^2 \nu^2 t^2) c_1 \right. \\ &\quad \left. + \Upsilon_2((1+\mu t^2)^2 - 12(1+6\mu\nu)\mu^2 \nu^2 t^2) c_2 - 72\mu^2 \nu^4 t^2 \right], \end{aligned} \quad (22)$$

$$\begin{aligned} p_m &= \frac{1}{216(1+\mu t^2)^2} \left[\frac{2\sqrt{6\mu}(1+\mu t^2)\mu \nu^2 t}{\left(\frac{\mu \nu t^2}{(1+\mu t^2)^2}\right)^{\frac{3}{2}}} + 648\mu \nu^2 t^2 - \frac{9}{\mu \nu^2} \right. \\ &\quad \times \left[\Upsilon_1((1+\mu t^2)^2 - 4(1+\mu t^2)(1-6\mu\nu)^2 \mu^2 \nu^3 t + 12 \right. \\ &\quad \times (-1+6\mu\nu)\mu^2 \nu^2 t^2) c_1 + \Upsilon_2((1+\mu t^2)^2 - 4(1+\mu t^2) \\ &\quad \times (\mu\nu + 6\mu\nu^2)^2 \mu \nu t - 12(1+6\mu\nu)\mu^2 \nu^2 t^2) c_2 \left. \right] \left. \right]. \end{aligned} \quad (23)$$

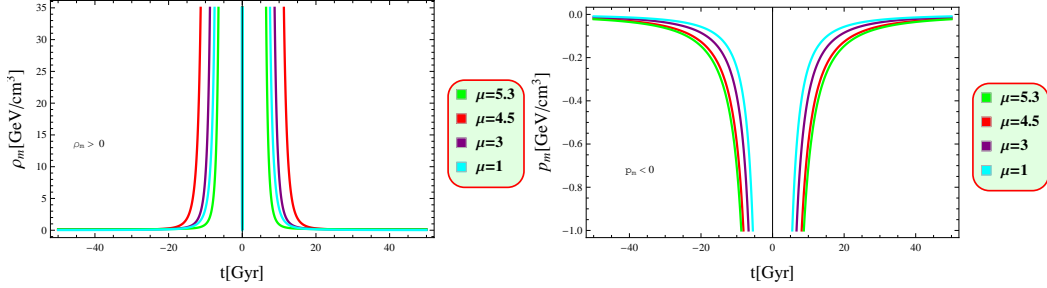


Figure 5: Profile of energy density and pressure versus cosmic time.

Here,

$$\Upsilon_1 = \exp\left(\frac{6(1 - 6\mu\nu)\mu^2\nu^2t^2}{(1 + \mu t^2)^2}\right), \quad \Upsilon_2 = \exp\left(\frac{6(1 + 6\mu\nu)\mu^2\nu^2t^2}{(1 + \mu t^2)^2}\right).$$

The graphical representation of energy density and pressure is depicted in Figure 5, which exhibits a positive trajectory for energy density and negative trend for pressure. These characteristics are crucial in understanding the dynamics of DE models.

3.5 Analysis of State Parameter

In this section, we discuss the physical attributes of different cosmic parameters. The EoS parameter ($\omega = \frac{p}{\rho}$) can be categorized into different stages of the cosmic development. The matter-dominated regions such as dust, radiative fluid and stiff matter regions are determined by $\omega = 0, \frac{1}{3}, 1$, respectively. Whereas the vacuum, phantom and quintessence cosmic phases are represented by $\omega = -1, \omega < -1$ and $-\frac{1}{3} < \omega < -1$, respectively [73]. The EoS parameter corresponding to the reconstructed $f(\mathcal{Q})$ gravity model is obtained as

$$\begin{aligned} \omega = & \frac{2}{9(\mu\nu)^{\frac{5}{2}}(1 + \mu t^2)^3 t^3} \left[\frac{1}{\Upsilon_1} ((1 + \mu t^2)^2 + 12(-1 + 6\mu\nu)\mu^2\nu^2 t^2) c_1 \right. \\ & \left. + \frac{1}{\Upsilon_2} ((1 + \mu t^2)^2 - 12(1 + 6\mu\nu)\mu^2\nu^2 t^2) c_2 - 72\mu\nu^3 t^2 \right]. \end{aligned} \quad (24)$$

The EoS parameter maintains a symmetrical behavior before and after the bounce point, preventing the occurrence of singularities during the bounce

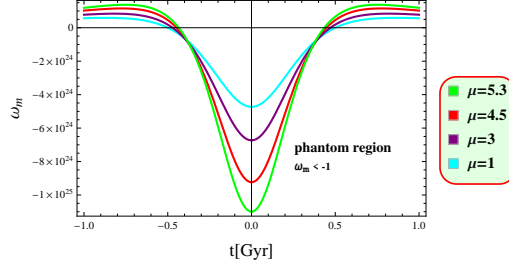


Figure 6: Plot of EoS parameter versus cosmic time.

Table 3: **Types of Energy Conditions**

Energy Conditions	Perfect Fluid
NEC	$\rho_m + p_m \geq 0$
SECs	$(n-3)\rho_m + (n-1)p_m, \rho_m + p_m \geq 0$
DECs	$\rho_m \geq p_m $
WECs	$\rho_m \geq 0, \rho_m + p_m \geq 0$

phases as shown in Figure 6. This ensures a smooth transition through the bounce phase as the EoS parameter does not approach to infinity at any point. Furthermore, the trajectory of the EoS parameter falls in the phantom region. This characterizes the dynamic transformation in the nature of dark matter and DE during the crucial phases in our universe.

3.6 Dynamics of Energy Conditions

The ECs are essential for the evolution of geodesic structures that are space-like, time-like, or light-like and figure out the singularity of spacetime. These constraints are helpful to comprehend the cosmic geometry and their relationships to the EMT. These are classified into four categories as NEC, WECs, SECs and DEC. Different forms of ECs are given in Table 3. Here, we explore the graphical representation of these energy constraints for the reconstructed $f(Q)$ model. By examining these ECs, we can determine the characteristics of cosmic geometries and their relationship to EMT. Violation of the null energy condition yields the violation of all ECs [74]. Using

Eqs.(22) and (23), we have

$$\begin{aligned}
\rho_m + p_m &= \frac{1}{24(1 + \mu t^2)^2 \mu \nu^2} \left[\Upsilon_1((1 + \mu t^2)^2 + 12(6\mu\nu - 1)\mu^2\nu^2 t^2) c_1 \right. \\
&+ \Upsilon_2((1 + \mu t^2)^2 - 12(1 + 6\mu\nu)\mu^2\nu^2 t^2) c_2 - 72\mu^2\nu^4 t^2 \left. \right] \\
&+ \frac{1}{216(1 + \mu t^2)^2} \left[\frac{2\sqrt{6\mu\nu^2}(1 + \mu t^2)\mu\nu t}{\left(\frac{\mu\nu t^2}{(1 + \mu t^2)^2}\right)^{\frac{3}{2}}} - \frac{9}{\mu\nu^2} \left[\Upsilon_1((1 + \mu t^2)^2 \right. \right. \\
&- 4(1 + \mu t^2)(1 - 6\mu\nu)^2\mu^2\nu^3 t + 12(-1 + 6\mu\nu)\mu^2\nu^2 t^2) c_1 + \Upsilon_2 \\
&\times ((1 + \mu t^2)^2 - 4(1 + \mu t^2)(\mu\nu + 6\mu\nu^2)^2\mu\nu t + 648\mu\nu^2 t^2 \\
&- 12(1 + 6\mu\nu)\mu^2\nu^2 t^2) c_2 \left. \right] \left. \right], \tag{25}
\end{aligned}$$

$$\begin{aligned}
\rho_m + 3p_m &= \frac{1}{24(1 + \mu t^2)^2 \mu \nu^2} \left[+ \Upsilon_1((1 + \mu t^2)^2 + 12(6\mu\nu - 1) \right. \\
&\times \mu^2\nu^2 t^2) c_1 + \Upsilon_2((1 + \mu t^2)^2 - 12(1 + 6\mu\nu)\mu^2\nu^2 t^2) c_2 \\
&- 72\mu^2\nu^4 t^2 \left. \right] + 3 \left[\frac{1}{216(1 + \mu t^2)^2} \left[\frac{2\sqrt{6\mu\nu^2}(1 + \mu t^2)\mu\nu t}{\left(\frac{\mu\nu t^2}{(1 + \mu t^2)^2}\right)^{\frac{3}{2}}} \right. \right. \\
&- \frac{9}{\mu\nu^2} \left[\Upsilon_1((1 + \mu t^2)^2 - 4(1 + \mu t^2)(1 - 6\mu\nu)^2\mu^2\nu^3 t \right. \\
&+ 12(-1 + 6\mu\nu)\mu^2\nu^2 t^2) c_1 + \Upsilon_2((1 + \mu t^2)^2 - 4 \\
&\times (1 + \mu t^2)(\mu\nu + 6\mu\nu^2)^2\mu\nu t - 12(1 + 6\mu\nu)\mu^2\nu^2 t^2) c_2 \left. \right] \\
&+ 648\mu\nu^2 t^2 \left. \right] \left. \right], \tag{26}
\end{aligned}$$

$$\begin{aligned}
\rho_m - p_m &= \frac{1}{24(1 + \mu t^2)^2 \mu \nu^2} \left[- 72\mu^2\nu^4 t^2 + \Upsilon_1((1 + \mu t^2)^2 + 12 \right. \\
&\times (6\mu\nu - 1)\mu^2\nu^2 t^2) c_1 + \Upsilon_2((1 + \mu t^2)^2 - 12(1 + 6\mu\nu) \\
&\times \mu^2\nu^2 t^2) c_2 \left. \right] - \frac{1}{216(1 + \mu t^2)^2} \left[\frac{2\sqrt{6\mu\nu^2}(1 + \mu t^2)\mu\nu t}{\left(\frac{\mu\nu t^2}{(1 + \mu t^2)^2}\right)^{\frac{3}{2}}} \right. \\
&- \frac{9}{\mu\nu^2} \left[\Upsilon_1((1 + \mu t^2)^2 - 4(1 + \mu t^2)(1 - 6\mu\nu)^2\mu^2\nu^3 t \right. \\
&+ 12(-1 + 6\mu\nu)\mu^2\nu^2 t^2) c_1 + \Upsilon_2((1 + \mu t^2)^2
\end{aligned}$$

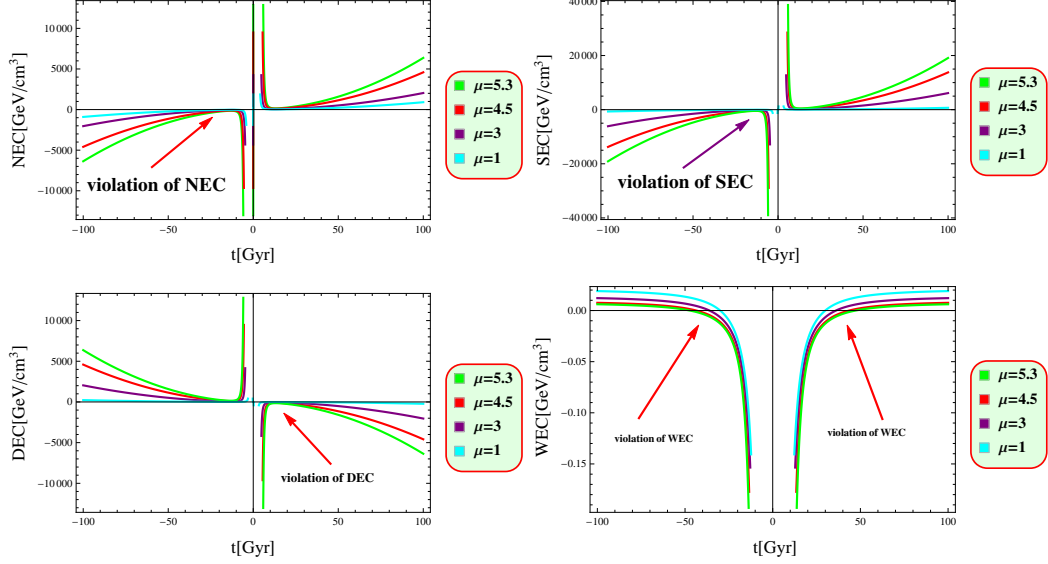


Figure 7: Behavior of energy conditions corresponding to cosmic time.

$$\begin{aligned}
& - \left[4(1 + \mu t^2)(\mu\nu + 6\mu\nu^2)^2\mu\nu t - 12(1 + 6\mu\nu)\mu^2\nu^2 t^2 \right] \\
& + 648\mu\nu^2 t^2 \Big]. \tag{27}
\end{aligned}$$

Figure 7 shows that there is no singularity in the vicinity of the bouncing point as energy constraints are negative near the bounce, providing strong indication of a violation of these ECs. In our analysis, the violation of the ECs interpreted to achieve a non-singular bounce that allows the universe to transition from a contracting phase to an expanding phase without encountering a singularity. Furthermore, it is important to note that such violations are localized in time and are confined to the immediate vicinity of the bounce. They do not extend to regions away from the bounce epoch, where the DEC's are restored which ensure that the model remains physically viable in the broader context.

4 Second Law of Thermodynamics

This analysis examines the second law of thermodynamics in the context of $f(\mathcal{Q})$ gravity. According to this law, the total entropy of the universe must increase over time. The total entropy comprises the entropy of matter in the universe (S_{in}) and the entropy on the boundary of the horizon (S_{on}). The units for entropy are Joules per Kelvin (JK^{-1}). It is assumed that the boundary of the universe is delimited by the radius of the apparent horizon, which can be determined using the Hubble parameter mentioned in Eq.(12).

$$R_h = \frac{1}{H} = \frac{\mu t^2 + 1}{t\mu\nu}. \quad (28)$$

In cosmology, the entropy of the horizon is associated with the horizon surface area as

$$A = 4\pi R_h^2 = \frac{4\pi(\mu t^2 + 1)^2}{t^2\mu^2\nu^2}. \quad (29)$$

By applying the Bekenstein-Hawking formulation, the entropy value at the horizon boundary is calculated as

$$S_{on} = \frac{K_b c^3}{G\hbar} \left[\frac{\pi(\mu t^2 + 1)^2}{t^2\mu^2\nu^2} \right], \quad (30)$$

where K_b is the Boltzmann constant and $\frac{G\hbar}{c^3} = L_p$ is the Planck's length. The time derivative of S_{on} turns out to be

$$\dot{S}_{on} = \frac{2K_b\pi}{L_p\mu^2\nu^2} \left(\mu^2 t - \frac{1}{t^3} \right). \quad (31)$$

It is noted that $\dot{S}_{on} > 0$ only when $\mu > \frac{1}{t^2}$.

Using the Gibbs relation, the value of entropy in the boundary of the horizon is obtained as

$$T_h dS_{in} = d(\rho_m V) + p_m dV, \quad (32)$$

where T_h is the Hawking temperature on the boundary of the horizon. The unit for Hawking temperature is considered as Kelvin (K). The volume inside the horizon is given by

$$V = \frac{4\pi}{3} \left(\frac{\mu t^2 + 1}{t\mu\nu} \right)^3. \quad (33)$$

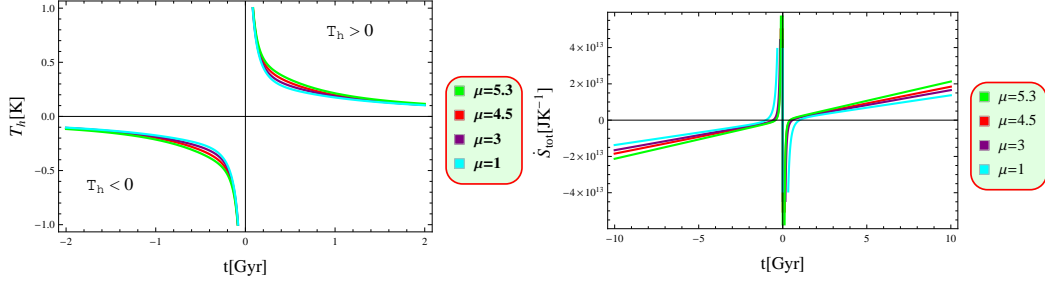


Figure 8: The evolution of total entropy and temperature versus t .

Differentiating Eq.(32) with respect to time t , we get

$$\begin{aligned}
 T_h \dot{S}_{in} = & \frac{4\pi}{3} \frac{(1 + \mu t^2)^3}{(\mu \nu t)^3} \times \frac{t\mu}{6\mu\nu^2(1 + \mu t^2)^2} \left[-36\mu\nu^4 + \frac{1}{(1 + \mu t^2)^3} \right. \\
 & \times \Upsilon_1 [(1 + \mu t^2)^4 - 36\mu^3 t^2 (1 - 6\mu\nu)\nu^4 + 216\mu^4 \nu^5 t^2 \\
 & \times (1 - 6\mu\nu) + 3\mu(-1 - 6\mu\nu + 3\mu t^2(1 + 2\mu\nu))(\nu + \mu t^2 \nu)^2 \\
 & + 36\mu^2(\nu + \mu t^2 \nu)^3] c_1 + \Upsilon_2 [1 + 72\mu^2 \nu^5 t^2 \\
 & \left. + \mu(t^2 + 24\mu^2 \nu^4 t + 2(-3 - 18\mu\nu + \mu^2 \nu t))\right] c_2 \Big] \quad (34)
 \end{aligned}$$

Hawking temperature is positive and can be calculated as

$$T_h = \frac{1}{2\pi R_h} \left(1 - \frac{\dot{R}_h}{2H R_h} \right) = \frac{\mu \nu t}{2\pi(1 + t^2 \mu)} \left[1 + \frac{1 - \mu t^2}{2\mu \nu t^2} \right]. \quad (35)$$

Since $S_{in} > 0$, the total entropy should not decrease in terms of time evolution. Thus, the second law of thermodynamics holds if the following condition is satisfied

$$\dot{S}_{tot} = \dot{S}_{on} + \dot{S}_{in} \geq 0. \quad (36)$$

Figure 8 shows that the total entropy of the universe increases near the bounce over time. Furthermore, the model indicates that the Hawking temperature is very high after the bouncing time.

5 Conclusions

In recent decades, researchers have faced challenges regarding the origin and development of the universe due to the limited observational data. As a

result, cosmologists have been studying bouncing cosmology as an alternative approach to address the inflationary problem and singularities in the big bang model [74]. This strategy becomes relevant when dealing with uncertainties related to early singularities. Nonsingular bouncing solutions play a crucial role in the early universe cosmology and it is essential to explore various facts of these solutions. The primary aim of this research is to determine the nature of nonsingular bounce. In this context, we have reconstructed the functional form of $f(\mathcal{Q})$ gravity, where \mathcal{Q} characterizes the gravitational interaction. The key results of our study are outlined as follows.

- The scale factor shows that the universe transits from contracting to expansion phase as it is monotonically decreasing before the bounce and increasing after the bounce. Also, it maintains its minimum value before and after the bouncing spot (Figure 1).
- The Hubble parameter becomes negative prior to the bounce point, signifying a contracting universe. This becomes zero as the cosmos approaches to the bounce point. As the universe transitions into the post-bounce phase, it takes on a positive value, indicating that the cosmos undergoes the expansionary phase. (Figure 2).
- Different values of the parameters μ and ν facilitate the shift from a contraction to an expansion in the present-day universe (Tables 1 and 2).
- The time derivative of the Hubble parameter shows that the cosmos transits from a contracting to an expanding state in the vicinity of the bounce point, which occurs in the cosmic time interval of -0.5 to 0.5 (Figure 3).
- The deceleration parameter demonstrates that the universe is undergoing an expansion phase as it is negative before and after the bounce (Figure 4).
- The positive energy density and negative pressure indicate that the universe is currently in an expanding state (Figure 5).
- The EoS parameter suggests that the universe is in the phantom era, confirming the cosmic expansion (Figure 6).

- The violation of all the ECs leads to the accelerated expansion (Figure 7).
- We have found that our reconstructed model attains high temperature at the bouncing point and exhibits an increasing behavior of total entropy over time (Figure 8).

The second law of thermodynamic plays a crucial role in bouncing cosmology and models of the accelerated expansion. Any viable cosmological model must adhere to this thermodynamic principle. This imposes constraints on the behavior of dark matter and DE throughout the cycles of contraction and expansion, ensuring that entropy consistently increases. We have explored the validity of the second law of thermodynamics corresponding to FRW universe bounded by a horizon. Our results indicate that the total entropy increases as the universe approaches to the bounce point and total entropy tends to infinity at the bounce point. We concluded an increasing behavior of the total entropy over time, reflecting the progression towards thermodynamic equilibrium.

Finally, we have compared our findings with Λ CDM model and found that all ECs are violated when the bouncing requirements are met. This behavior is not compatible with Λ CDM as in Λ CDM only SEC is violated [75]. Both the observed accelerated expansion and the predictions of the Λ CDM model align with this behavior [76]. It is worthwhile to mention here that the reconstruction model satisfies all the necessary conditions for a successful non-singular stable bouncing model.

Appendix X: Computation of $\mathcal{Q} = -\mathcal{Q}_{\xi\alpha\beta}\mathcal{P}^{\xi\alpha\beta}$

Non-metricity tensor is expressed as

$$\mathcal{Q} = -g^{\alpha\beta}(L_{\phi\alpha}^{\xi}L_{\beta\xi}^{\phi} - L_{\phi\xi}^{\xi}L_{\alpha\beta}^{\phi}), \quad (\text{X1})$$

where

$$L_{\phi\alpha}^{\xi} = -\frac{1}{2}g^{\xi\eta}(\mathcal{Q}_{\alpha\phi\eta} + \mathcal{Q}_{\phi\eta\alpha} - \mathcal{Q}_{\eta\phi\alpha}), \quad (\text{X2})$$

$$L_{\beta\xi}^{\phi} = -\frac{1}{2}g^{\phi\tau}(\mathcal{Q}_{\xi\beta\tau} + \mathcal{Q}_{\beta\xi\tau} - \mathcal{Q}_{\tau\beta\xi}), \quad (\text{X3})$$

$$L_{\phi\xi}^{\xi} = -\frac{1}{2}g^{\xi\eta}(\mathcal{Q}_{\xi\phi\eta} + \mathcal{Q}_{\phi\eta\xi} - \mathcal{Q}_{\eta\xi\phi}), \quad (\text{X4})$$

$$L_{\alpha\beta}^{\phi} = -\frac{1}{2}g^{\phi\tau}(\mathcal{Q}_{\beta\alpha\tau} + \mathcal{Q}_{\alpha\tau\beta} - \mathcal{Q}_{\tau\alpha\beta}). \quad (\text{X5})$$

Therefore, we get

$$-g^{\alpha\beta}L_{\phi\alpha}^{\xi}L_{\beta\xi}^{\mu} = -\frac{1}{4}(2\mathcal{Q}^{\xi\beta\tau}\mathcal{Q}_{\tau\xi\beta} - \mathcal{Q}^{\xi\beta\tau}\mathcal{Q}_{\xi\beta\tau}), \quad (\text{X6})$$

$$g^{\alpha\beta}L_{\phi\xi}^{\xi}L_{\alpha\beta}^{\phi} = \frac{1}{4}g^{\alpha\beta}g^{\mu\eta}\mathcal{Q}_{\phi}(\mathcal{Q}_{\beta\alpha\eta} + \mathcal{Q}_{\alpha\eta\beta} - \mathcal{Q}_{\eta\beta\alpha}), \quad (\text{X7})$$

$$\begin{aligned} \mathcal{Q} &= -\frac{1}{4}(-\mathcal{Q}^{\xi\beta\tau}\mathcal{Q}_{\xi\beta\tau} + 2\mathcal{Q}^{\xi\beta\tau}\mathcal{Q}_{\tau\xi\beta} - 2\mathcal{Q}^{\xi}\tilde{\mathcal{Q}}_{\xi} \\ &\quad - 2\mathcal{Q}^{\xi}\mathcal{Q}_{\xi}). \end{aligned} \quad (\text{X8})$$

Using Eq.(20), we have

$$\begin{aligned} \mathcal{P}^{\xi\alpha\beta} &= \frac{1}{4}\left[-\mathcal{Q}^{\xi\alpha\beta} + \mathcal{Q}^{\alpha\xi\beta} + \mathcal{Q}^{\beta\xi\alpha} + \mathcal{Q}^{\xi}g^{\alpha\beta} - \tilde{\mathcal{Q}}^{\xi}g^{\alpha\beta} - \frac{1}{2}(g^{\xi\alpha}\mathcal{Q}^{\beta} \right. \\ &\quad \left. + g^{\xi\beta}\mathcal{Q}^{\alpha})\right], \end{aligned} \quad (\text{X9})$$

$$\begin{aligned} -\mathcal{Q}_{\xi\alpha\beta}\mathcal{P}^{\xi\alpha\beta} &= -\frac{1}{4}(-\mathcal{Q}^{\xi\alpha\beta}\mathcal{Q}_{\xi\alpha\beta} + 2\mathcal{Q}_{\xi\alpha\beta}\mathcal{Q}^{\alpha\xi\beta} + \mathcal{Q}^{\xi}\mathcal{Q}_{\xi} - 2\mathcal{Q}_{\xi}\tilde{\mathcal{Q}}^{\xi}) \\ &= \mathcal{Q}. \end{aligned} \quad (\text{X10})$$

Appendix Y: Calculation of $\delta\mathcal{Q}$

We list all the non-metricity tensors that will be used prior to presenting the detailed variation of the non-metricity scalar, \mathcal{Q} .

$$\mathcal{Q}_{\xi\alpha\beta} = \nabla_{\xi}g_{\alpha\beta}, \quad (\text{Y1})$$

$$\mathcal{Q}_{\alpha\beta}^{\xi} = g^{\xi\eta}\mathcal{Q}_{\eta\alpha\beta} = g^{\xi\eta}\nabla_{\eta}g_{\alpha\beta} = \nabla^{\xi}g_{\alpha\beta}, \quad (\text{Y2})$$

$$\mathcal{Q}_{\xi}^{\alpha\beta} = g^{\alpha\eta}\mathcal{Q}_{\xi\eta\beta} = g^{\alpha\eta}\nabla_{\xi}g_{\eta\beta} = -g_{\eta\beta}\nabla_{\xi}g^{\alpha\eta}, \quad (\text{Y3})$$

$$\mathcal{Q}_{\xi\alpha}^{\beta} = g^{\beta\eta}\mathcal{Q}_{\xi\alpha\eta} = g^{\beta\eta}\nabla_{\xi}g_{\alpha\eta} = -g_{\alpha\eta}\nabla_{\xi}g^{\beta\eta}, \quad (\text{Y4})$$

$$\mathcal{Q}_{\beta}^{\xi\alpha} = g^{\xi\eta}g^{\alpha\tau}\nabla_{\eta}g_{\tau\beta} = g^{\alpha\tau}\nabla^{\xi}g_{\tau\beta} = -g_{\tau\beta}\nabla^{\xi}g^{\alpha\tau}, \quad (\text{Y5})$$

$$\mathcal{Q}_{\alpha}^{\xi\beta} = g^{\xi\nu}g^{\beta\tau}\nabla_{\eta}g_{\alpha\tau} = g^{\beta\tau}\nabla^{\xi}g_{\alpha\tau} = -g_{\alpha\tau}\nabla^{\xi}g^{\beta\tau}, \quad (\text{Y6})$$

$$\mathcal{Q}_{\xi}^{\alpha\beta} = g^{\alpha\tau}g^{\beta\eta}\nabla_{\xi}g_{\tau\eta} = -g^{\alpha\tau}g_{\tau\eta}\nabla_{\xi}g^{\beta\eta} = -\nabla_{\xi}g^{\alpha\beta}, \quad (\text{Y7})$$

$$\mathcal{Q}^{\xi\alpha\beta} = -\nabla^\xi g_{\alpha\beta}. \quad (\text{Y8})$$

Using Eqs.(X6) and (X7), we obtain

$$\begin{aligned} \delta\mathcal{Q} &= -\frac{1}{4}\delta\left(-\mathcal{Q}^{\xi\beta\tau}\mathcal{Q}_{\xi\beta\tau}+2\mathcal{Q}^{\xi\beta\tau}\mathcal{Q}_{\tau\xi\beta}-2\mathcal{Q}^\xi\tilde{\mathcal{Q}}_\xi+2\mathcal{Q}^\xi\mathcal{Q}_\xi\right), \\ &= -\frac{1}{4}\left(-\delta\mathcal{Q}^{\xi\beta\tau}\mathcal{Q}_{\xi\beta\tau}-\mathcal{Q}^{\xi\beta\tau}\delta\mathcal{Q}_{\xi\beta\tau}+2\delta\mathcal{Q}^{\xi\beta\tau}\mathcal{Q}_{\tau\xi\beta}\right. \\ &\quad +2\mathcal{Q}^{\xi\beta\tau}\delta\mathcal{Q}_{\tau\xi\beta}-2\delta\mathcal{Q}^\xi\tilde{\mathcal{Q}}_\xi-2\mathcal{Q}^\xi\delta\tilde{\mathcal{Q}}_\xi+\delta\mathcal{Q}^\xi\mathcal{Q}_\xi+\mathcal{Q}^\xi\delta\mathcal{Q}_\xi\Big), \\ &= -\frac{1}{4}\left[\mathcal{Q}_{\xi\beta\tau}\nabla^\xi\delta g^{\beta\tau}-\mathcal{Q}^{\xi\beta\tau}\nabla_\xi\delta g_{\beta\tau}-2\mathcal{Q}_{\tau\xi\beta}\nabla^\xi\delta g^{\beta\tau}+2\mathcal{Q}^{\xi\beta\tau}\nabla_\tau\delta g_{\xi\beta}\right. \\ &\quad +2\tilde{\mathcal{Q}}_\tau\nabla^\tau g^{\alpha\beta}\delta g_{\alpha\beta}+2\tilde{\mathcal{Q}}_\tau g_{\alpha\beta}\nabla^\tau\delta g^{\alpha\beta}-2\mathcal{Q}^\tau\nabla^\nu\delta g_{\tau\eta}-\mathcal{Q}_\tau\nabla^\tau g^{\alpha\beta}\delta g_{\alpha\beta} \\ &\quad \left.-\mathcal{Q}_\tau g_{\alpha\beta}\nabla^\tau\delta g^{\alpha\beta}-\mathcal{Q}^\tau\nabla_\tau g^{\alpha\beta}\delta g_{\alpha\beta}-\mathcal{Q}^\tau g_{\alpha\beta}\nabla_\tau\delta g^{\alpha\beta}\right]. \end{aligned} \quad (\text{Y9})$$

Here, We use the following equations as

$$\delta g_{\alpha\beta} = -g_{\alpha\xi}\delta g^{\xi\nu}g_{\eta\beta}, \quad (\text{Y10})$$

$$\begin{aligned} -\mathcal{Q}^{\xi\beta\tau}\nabla_\xi\delta g_{\beta\tau} &= -\mathcal{Q}^{\xi\beta\tau}\nabla_\xi(-g_{\beta\eta}\delta g^{\nu\vartheta}g_{\vartheta\tau}) \\ &= 2\mathcal{Q}^{\xi\psi}_\beta\mathcal{Q}_{\xi\psi\alpha}\delta g^{\alpha\beta}+\mathcal{Q}_{\xi\beta\tau}\nabla^\xi g^{\beta\tau}, \end{aligned} \quad (\text{Y11})$$

$$2\mathcal{Q}^{\xi\beta\tau}\nabla_\tau\delta g_{\xi\beta} = -4\mathcal{Q}_\alpha^{\psi\tau}\mathcal{Q}_{\tau\psi\beta}\delta g^{\alpha\beta}-2\mathcal{Q}_{\beta\tau\xi}\nabla^\xi g^{\beta\tau}, \quad (\text{Y12})$$

$$\begin{aligned} -2\mathcal{Q}^\tau\nabla^\eta\delta g_{\tau\eta} &= 2\mathcal{Q}^\xi\mathcal{Q}_{\beta\xi\alpha}\delta g^{\alpha\beta}+2\mathcal{Q}_\alpha\tilde{\mathcal{Q}}_\beta\delta g^{\alpha\beta} \\ &\quad +2\mathcal{Q}_\beta g_{\xi\tau}\nabla^\xi g^{\beta\tau}. \end{aligned} \quad (\text{Y13})$$

Thus, Eq.(Y9) becomes

$$\delta\mathcal{Q} = 2\mathcal{P}_{\xi\beta\tau}\nabla^\xi\delta g^{\beta\tau}-(\mathcal{P}_{\alpha\xi\eta}\mathcal{Q}_\beta^{\xi\eta}-2\mathcal{Q}^{\xi\eta}_\alpha\mathcal{P}_{\alpha\eta\beta})\delta g^{\alpha\beta}, \quad (\text{Y14})$$

where

$$\begin{aligned} 2\mathcal{P}_{\xi\beta\tau} &= -\frac{1}{4}\left[2\mathcal{Q}_{\xi\beta\tau}-2\mathcal{Q}_{\tau\xi\beta}-2\mathcal{Q}_{\beta\tau\xi}+2\mathcal{Q}_\beta g_{\xi\tau}+2\tilde{\mathcal{Q}}_\xi g_{\beta\tau}\right. \\ &\quad \left.-2\mathcal{Q}_\xi g_{\beta\tau}\right], \end{aligned} \quad (\text{Y15})$$

$$\begin{aligned} 4(\mathcal{P}_{\alpha\xi\eta}\mathcal{Q}_\beta^{\xi\eta}-2\mathcal{Q}^{\xi\eta}_\alpha\mathcal{P}_{\alpha\eta\beta}) &= 2\mathcal{Q}^{\xi\eta}_\beta\mathcal{Q}_{\xi\eta\alpha}-4\mathcal{Q}_\alpha^{\xi\eta}\mathcal{Q}_{\eta\xi\beta} \\ &\quad +2\tilde{\mathcal{Q}}^\xi\mathcal{Q}_{\xi\alpha\beta}+2\mathcal{Q}^\xi\mathcal{Q}_{\beta\xi\alpha}+2\mathcal{Q}_\alpha\tilde{\mathcal{Q}}_\beta-\mathcal{Q}^\xi\mathcal{Q}_{\xi\alpha\beta}. \end{aligned} \quad (\text{Y16})$$

Appendix Z: Calculation of $\mathcal{Q} = 6H^2$

From Eq.(X10), we have

$$\mathcal{Q} = -\frac{1}{4}(-\mathcal{Q}_{\xi\alpha\beta}\mathcal{Q}^{\xi\alpha\beta} + 2\mathcal{Q}_{\xi\alpha\beta}\mathcal{Q}^{\alpha\xi\beta} + \mathcal{Q}_{\xi}\mathcal{Q}^{\xi} - 2\mathcal{Q}_{\xi}\tilde{\mathcal{Q}}^{\xi}). \quad (\text{Z1})$$

For the case of FRW metric, we get

$$-\mathcal{Q}_{\xi\alpha\beta}\mathcal{Q}^{\xi\alpha\beta} = \nabla_{\xi}g_{\alpha\beta}\nabla^{\xi}g^{\alpha\beta} = 4(3H^2), \quad (\text{Z2})$$

$$\mathcal{Q}_{\xi\alpha\beta}\mathcal{Q}^{\xi\alpha\beta} = \nabla_{\xi}g_{\alpha\beta}\nabla^{\xi}g^{\alpha\beta} = -4(3H^2), \quad (\text{Z3})$$

$$\mathcal{Q}_{\xi}\mathcal{Q}^{\xi} = (g_{\tau\alpha}\nabla_{\xi}g^{\tau\alpha})(g_{\psi\beta}\nabla^{\xi}g^{\psi\beta}) = -4(3H)^2, \quad (\text{Z4})$$

$$\mathcal{Q}_{\xi}\tilde{\mathcal{Q}}^{\xi} = (g_{\alpha\tau}\nabla_{\xi}g^{\alpha\tau})(\nabla_{\eta}g^{\xi\eta}) = -4(T^2 + 3H^2). \quad (\text{Z5})$$

Using Eqs.(Z2) -(Z5) in (Z1), we obtain

$$\mathcal{Q} = -\frac{1}{4}\left[12H^2 - 36H^2\right] = 6H^2. \quad (\text{Z6})$$

Data Availability Statement: No data was used for the research described in this paper.

References

- [1] Carroll, S.M.: Living Rev. Relativ. **4**(2001)1.
- [2] Cognola, G. et al.: Phys. Rev. D **77**(2008)046009.
- [3] Felice, A.D. and Tsujikawa S.R.: Living Rev. Relativ. **13**(2010)161.
- [4] Linder, E.V.: Phys. Rev. D **81**(2010)127301.
- [5] Cai, Y.F. et al.: Prog. Phys. **79**(2016)106901.
- [6] Nojiri, S., Odintsov, S.D. and Oikonomou, V.K.: Phys. Rept. **692**(2017)104.
- [7] Sharif, M., Gul, M.Z.: Eur. Phys. J. Plus **133**(2018)345.
- [8] Sharif, M., Gul, M.Z.: Int. J. Mod. Phys. D **28**(2019)1950054.

- [9] Sharif, M., Gul, M.Z.: Chin. J. Phys. **57**(2019)329.
- [10] Gul, M.Z. and Sharif, M.: New Astron. **106**(2024)102137.
- [11] Sharif, M., Gul, M.Z.: Ann. Phys. **465**(2024)169674.
- [12] Sharif, M., Gul, M.Z.: Phys. Scr. **99**(2024)065036.
- [13] Gul, M.Z., Sharif, M. and Hashim, I.: Phsys. Dark Universe **45**(2024)101537.
- [14] Gul, M.Z. and Sharif, M.: Phys. Scr. **99**(2024)055036.
- [15] Gul, M.Z. and Sharif, M.: Chin. J. Phys. **88**(2024)388.
- [16] Gul, M.Z., Sharif, M. and Kanwal, I.: New Astron. **109**(2024)102204.
- [17] Jimenez, J.B., Heisenberg, L. and Koivisto, S.T.: Phys. Rev. D **98**(2018)044048.
- [18] Lazkoz, R. et al.: Phys. Rev. D **100**(2019)104027.
- [19] Jimenez, J.B. et al.: Phys. Rev. D **101**(2020)103507.
- [20] Mandal, S. et al.: Phys. Rev. D **102**(2020)024057.
- [21] Bajardi, F., Vernieri, D. and Capozziello, S.: Eur. Phys. J. Plus **135**(2020)912.
- [22] Hassan, Z., Mandal, S. and Sahoo, P.K.: Fortschr. Phys. **69**(2021)2100023.
- [23] Solanki, R. et al.: Phys. Dark Universe **32**(2021)100820.
- [24] Esposito, F. et al.: Phys. Rev. D **105**(2022)084061.
- [25] Arora, S. Sahoo, P.K.: Ann. Phys. **534**(2022)2200233.
- [26] Albuquerque, I.S. and Frusciante, N.: Phys. Dark Universe **35**(2022)100980.
- [27] Sokoliuk, O. et al.: Mon. Not. R. Astron. Soc. **522**(2023)252.
- [28] Khyllep, W. et al.: Phys. Rev. D **107**(2023)044022.

- [29] Adeel, M. et al.: Mod. Phys. Lett. A **38**(2023)2350152.
- [30] Rani, S. et al.: Int. J. Geom. Methods Mod. Phys. **21**(2024)2450033.
- [31] Gul, M.Z. et al.: Eur. Phys. J. C **84**(2024)8.
- [32] Gul, M.Z., Sharif, M. and Arooj, A.: Fortschr. Phys. **72**(2024)2300221.
- [33] Gul, M.Z., Sharif, M. and Arooj, A.: Phys. Scr. **99**(2024)045006.
- [34] Gul, M.Z., Sharif, M. and Arooj, A.: Gen. Relativ. Gravit. **56**(2024)45.
- [35] Gul, M.Z. et al.: Eur. Phys. J. C **84**(2024)775.
- [36] Sharif, M., Gul, M. Z. and Fatima, N.: New Astron. **109**(2024)102211.
- [37] Sharif, M., Gul, M. Z. and Fatima, N.: Chin. J. Phys. **91**(2024)66.
- [38] Liddle, A.R.: J. High Energy Phys. **260**(1998)3.
- [39] Barragan, C., Olmo, G.J. and Helios, S.A.: Phys. Rev. D **80**(2009)024016.
- [40] Saaiddi, K., Aghamohammadi, A. and Hossienkhani, H.: Astrophys. Space Sci. **341**(2012)662.
- [41] Jawad, A. and Rani, S.: Astrophys. Space Sci. **359**(2015)23.
- [42] Shabani, H. and Ziaie, A.H.: Eur. Phys. J. C **78**(2018)397.
- [43] Aly, A.A.: Pramana **92**(2019)8.
- [44] Malik, A. and Shamir, M.F.: New Astron. **82**(2021)101460.
- [45] Shekh, S.H.: New Astron. **83**(2021)101464.
- [46] Ilyas, M. et al.: Indian J. Phys. **96**(2022)4017.
- [47] Zubair, M., Muneer, Q. and Waheed, S.: Int. J. Mod. Phys. D **31**(2022)2250092.
- [48] Bhardwaj, V.K. et al.: Can. J. Phys. **100**(2022)475.
- [49] Lohakare, S.V. et al.: Universe **8**(2022)636.

- [50] Dimakis, N. et al.: Eur. Phys. J. C **83**(2023)794.
- [51] Javed, F. et al.: Nucl. Phys. B **990**(2023)116180.
- [52] Javed, F. et al.: Fortschr. Phys. **2023**(2023)2200214.
- [53] Javed, F. et al.: Eur. Phys. J. C **83**(2023)1088.
- [54] Javed, F.: Ann. Phys. **458**(2023)169464.
- [55] Sharif, M., Gul, M.Z. and Fatima, N.: New Astron. **109** (2024)102211.
- [56] Sharif, M. and Gul, M.Z.: Phys. Scr. **96**(2021)025002.
- [57] Sharif, M. and Gul, M.Z.: Eur. Phys. J. Plus **136**(2021)503.
- [58] Sharif, M. and Gul, M.Z.: Phys. Scr. **96**(2021)125007.
- [59] Sharif, M. and Gul, M.Z.: Chin. J. Phys. **80**(2022)58.
- [60] Sharif, M. and Gul, M.Z.: Phys. Scr. **96**(2021)105001.
- [61] Gul, M.Z. and Sharif, M.: Universe **9**(2023)145.
- [62] Sharif, M. and Gul, M.Z.: Chin. J. Phys. **71**(2021)35.
- [63] Sharif, M. and Gul, M.Z.: Int. J. Mod. Phys. A **36**(2021)2150004.
- [64] Sharif, M. and Gul, M.Z.: Fortschr. Phys. **71**(2023)2200184;
- [65] Sharif, M. and Gul, M.Z.: Gen. Relative. Gravit. **55**(2023)10.
- [66] Sharif, M. and Gul, M.Z.: Phys. Scr. **98**(2023)035030.
- [67] Gul, M.Z., Sharif, M. and Afzal, A.: Chin. J. Phys. **89**(2024)1347.
- [68] Odintsov, S.D. and Oikonomou, V.K.: Phys. Rev. D **92**(2015)024016.
- [69] Shaily, Singh, J.K. and Singh, A.: Fortschritte der Physik **72**(2024)2300244.
- [70] Mandal, S., Wang, D. and Sahoo, P.K.: Phys. Rev. D **102**(2020)124029.
- [71] Banerjee, P., Garain, D. and Paul, S.: Astrophys. J. **910**(2021)23.

- [72] Cai Y.F. and Easson D.A.: *Astropart. Phys.* **8**(2012)020.
- [73] Gadbail, G.N., Mandal, S. and Sahoo, P.K.: *Phys.* **4**(2022)1403.
- [74] Bamba, K. et al.: *J. Cosmol. Astropart. Phys.* **2014**(2014)008.
- [75] Mandal, S. et al.: *Phys. Rev. D* **102**(2020)024057.
- [76] Aghanim, N. et al.: *Astron. Astrophys.* **641**(2020)6.